Video Article

A Comprehensive Procedure to Evaluate the *In Vivo* Performance of Cancer Nanomedicines

Jun Tang[1], Carlos Pérez-Medina[1,2], Yiming Zhao[2], Ahmad Sadique[1], Willem J. M. Mulder[2], Thomas Reiner[1]

[1]Department of Radiology, Memorial Sloan Kettering Cancer Center

[2]Translational and Molecular Imaging Institute, Icahn School of Medicine at Mount Sinai

Correspondence to: Jun Tang at jun.tang.mssm@gmail.com

URL: https://www.jove.com/video/55271
DOI: doi:10.3791/55271

Keywords: Cancer Research, Issue 121, nanomedicine, PET, radiolabeling, flow cytometry, liposome, molecular imaging, melanoma, immunocompetent mouse models

Date Published: 3/4/2017

Citation: Tang, J., Pérez-Medina, C., Zhao, Y., Sadique, A., Mulder, W.J., Reiner, T. A Comprehensive Procedure to Evaluate the *In Vivo* Performance of Cancer Nanomedicines. *J. Vis. Exp.* (121), e55271, doi:10.3791/55271 (2017).

Abstract

Inspired by the success of previous cancer nanomedicines in the clinic, researchers have generated a large number of novel formulations in the past decade. However, only a small number of nanomedicines have been approved for clinical use, whereas the majority of nanomedicines under clinical development have produced disappointing results. One major obstacle to the successful clinical translation of new cancer nanomedicines is the lack of an accurate understanding of their *in vivo* performance. This article features a rigorous procedure to characterize the *in vivo* behavior of nanomedicines in tumor-bearing mice at systemic, tissue, single-cell, and subcellular levels via the integration of positron emission tomography-computed tomography (PET-CT), radioactivity quantification methods, flow cytometry, and fluorescence microscopy. Using this approach, researchers can accurately evaluate novel nanoscale formulations in relevant mouse models of cancer. These protocols may have the ability to identify the most promising cancer nanomedicines with high translational potential or to aid in the optimization of cancer nanomedicines for future translation.

Video Link

The video component of this article can be found at https://www.jove.com/video/55271/

Introduction

Nanomedicine is shifting the paradigm of cancer treatment development[1]. Inspired by the tremendous clinical impact of previous cancer nanomedicines, such as liposome- and albumin-based nanotherapies[2,3], many novel formulations have been produced in the past decade. However, recent analyses of the clinical translation success of these cancer nanomedicines indicate that only a few of them have been approved for clinical use[4,5]. One major obstacle to the clinical translation of new cancer nanomedicines is their limited improvement of the therapeutic index compared with the direct administration of the free therapeutic compounds[6]. As such, accurate evaluation of the *in vivo* performance of nanomedicines at systemic, tissue, and cellular levels in preclinical animal models is essential to identify those with optimal therapeutic indices for future clinical translation.

Nanomaterials can be radiolabeled for quantitative characterization in living animals with positron emission tomography (PET) imaging, which has superb sensitivity and reproducibility among all clinical imaging modalities[7]. For example, ^{89}Zr-labeled long-circulating nanomedicines have been characterized in mouse models for cancer[8,9,10], as well as in other disease models[11]. In addition, the blood half-life and biodistribution of the nanomedicines can be extensively evaluated by using *ex vivo* radioactivity measurements in individual tissues[8]. Therefore, radiolabeling allows for the quantitative evaluation of nanomedicines at systemic and tissue levels.

Importantly, radiolabeled nanomedicines generally cannot be analyzed at the single-cell or subcellular levels due to the limited spatial resolution of the radioactive signal. Therefore, fluorescent labeling proves to be a complementary modality for the evaluation of nanoparticles with optical imaging techniques such as flow cytometry and fluorescence microscopy[12]. To this end, nanoparticles labeled with radioisotopes and fluorescent tags can be quantitatively evaluated *in vivo* by nuclear imaging and *ex vivo* by radioactivity counting, and they can also be extensively characterized at the cellular level by optical imaging.

Previously, we have developed modular procedures to incorporate radioactive and fluorescent labels into various nanoparticles, including high-density lipoprotein (HDL)[11], liposomes[9,10], polymeric nanoparticles, antibody fragments, and nanoemulsions[10,13]. These labeled nanoparticles have allowed for quantitative characterization in relevant animal models at different levels, which guided the optimization of these nanomaterials for their specific applications. In the current study, the aim is to use liposomal nanoparticles—the most established nanomedicine platform[14]—as an example to demonstrate comprehensive procedures to generate a dual-labeled nanoparticle and to thoroughly characterize it in a classic syngeneic melanoma B16-F10 mouse model[15]. From the results, we are confident this nanoparticle characterization approach can be adapted to evaluate other cancer nanomedicines in relevant mouse models.

Protocol

The procedure consists of the dual radioactive and fluorescent labeling of nanoparticles, *in vivo* PET-CT imaging, *ex vivo* biodistribution measurements, and *ex vivo* immunostaining and flow cytometry analyses. All animal experiments were approved by the Institutional Animal Care and Use Committee of Memorial Sloan Kettering Cancer Center.

1. Preparation of Dual-labeled Liposomes

NOTE: Syngeneic B16 melanoma tumors can be induced by injecting 300,000 B16-F10 cells into the back flanks of C57BL/6 mice under anesthesia from inhaling 2%-isoflurane-containing oxygen. Use sterile reagents and tools in a sterile workspace during surgery. After surgery, carefully observe the animals until their recovery from anesthesia. Put the animals back in their cages only when they regain full consciousness and mobility. House them in sterile rooms for animals with xenografted tumors. Tumors with a size of 300 mm^3 are ideal for nanoparticle characterization due to their pronounced enhanced permeability and retention effects (EPR), which can increase nanoparticle accumulation. The detailed protocols are provided below.

1. In a round-bottom flask, dissolve a mixture of 20 mg of lipids in 2 mL of chloroform containing 1,2-dipalmitoyl- *sn*-glycero-3-phophocholine (DPPC), cholesterol, 1,2-disearoyl- *sn*-glycero-3-phosphoethanolamine-poly(ethylene glycol)2000 (DSPE-PEG2000), DSPE-deferoxamine (DSPE-DFO) [8], and 1,1-diododecyl-3,3,3,3-tetramethylindodicarbocyanine-5,5-disulfonic acid (DiIC12[5]-DS) at molar ratios of 61.3%, 33.4%, 5, 0.2%, and 0.1%, respectively.
   NOTE: This lipid composition is very similar to the liposomal formulation of doxorubicin currently used in the clinic [2]. The resulting liposomes from our procedure will closely mimic the *in vivo* performance of the clinical nanomedicine.
2. Use a rotary evaporator to remove the organic solvent and form a thin lipid film at room temperature. Add 20 mL of PBS and sonicate for 30 min to generate liposomal nanoparticles by using a 3.8-mm sonication tip and an amplitude of 30 W, with sufficient cooling on ice.
3. Centrifuge the liposome solution at 4,000 x g for 10 min to remove the aggregates and wash the nanoparticles with PBS using centrifugal filtration (molecular weight cut-off (MWCO: 100 kDa) to remove free lipids and residual organic solvent. Concentrate the liposomes, which will remain in the top chamber, and transfer them to a new tube. The liposomes can be stored in a fridge in PBS for up to 1 week before the subsequent steps.
4. For quality control, characterize the liposomes by dynamic light scattering (DLS). Specifically, mix 50 µL of liposomes with 950 µL of PBS, and then transfer the mixture into the sizing cuvette. Place the cuvette in the analyzer and measure the particle sizes and their size distribution. The particle sizes and their size distribution (polydispersity index (PDI)) are expected to be 90 - 120 nm and 0.1 - 0.2, respectively.
5. For radiolabeling, mix the purified liposomes, equivalent to 2 mg of lipids, in PBS at a pH between 6.9 and 7.1 with 1 mCi ^{89}Zr-oxalate at 37 °C for 2 h in a 1.5-mL tube, (total volume: ~ 100 µL). Remove the free, unreacted ^{89}Zr by centrifugal filtration (MWCO = 100 kDa), similar to step 1.3. Wash the retentate with sterile PBS and dilute it to the desired volume. The radiochemical yield should be 80 - 95%.
   CAUTION! Working with radioactive materials is highly regulated. Institutions must be certificated and provide the necessary facilities, personnel training, and strict monitoring of radioactivity use. Researchers need to receive adequate training and wear personal protective equipment and dosimetry rings/badges when handling radioactivity.
6. Determine the radiochemical purity of the radiolabeled liposomes by size exclusion radio-HPLC, which typically should be over 98% [10]. Radiochemical purities lower than 95% are indicative of insufficient washing on step 1.5.
7. After radiolabeling, determine the size of the nanoparticles by dynamic light scattering. The size and PDI are expected to be within the same range as the measurements in step 1.4 [10].
   NOTE: If radioactive samples are not allowed in the flow cytometer or fluorescence microscope, non-radioactive ^{nat}Zr-oxalate can be used to label liposomes in step 1.5. These non-radioactive liposomes have identical characteristics to their radioactive analogs. A depiction of this procedure is provided in **Figure 2**.

2. *In Vivo* PET-CT Imaging and Biodistribution of Dual-labeled Liposomes

1. Inject about 100 µL of dual-labeled liposomes with about 300 µCi of radioactivity into restrained melanoma mice (C57BL/6, female, 10 - 16 weeks old) through their tail veins, at about 10 mCi ^{89}Zr/kg body weight.
2. To determine the half-life, draw blood from the tail vein from anesthetized animals under 2% isoflurane-containing oxygen using 28-G insulin syringes. Collect the blood (10 - 20 µL) in pre-weighed tubes at 2 min, 15 min, 1 h, 4 h, 8 h, 24 h, and 48 h after injection. Weigh the blood by difference, determine radioactivity content using a gamma counter, and calculate radioactivity concentration as percentage of injected dose per gram (%ID/g).
   NOTE: Perform the procedure in a room equipped with an anesthesia system, recovery cages, heating, and a biohazard hood. Make sure that the animals fully recover and gain normal mobility after the procedure before transferring them from recovery cages to holding cages. House the tumor-bearing animals in rooms designated for animals administered with radioactive materials.
3. 24 or 48 h after the injection of the liposomes, image the mice in a small-animal MicroPET-CT scanner [10]. Place the anesthetized animal horizontally on its belly and keep it anesthetized. Administer 2% isoflurane-oxygen through a nose cone. Apply ophthalmic ointment to its eyes before the scan to prevent them from drying.
4. Perform a whole-body PET static scan recording at least 50 million coincident events, with an approximate duration of 15 min. Set the energy and coincidence timing window at 350-700 keV and 6 ns, respectively. Afterwards, perform a 5-min computed tomography (CT) scan. Set the X-ray tube to a voltage of 80 kV and a current of 500 µA; the CT scan uses 120 rotational steps for a total of 220 degrees, with approximately 145 ms per frame [10].
5. After the PET-CT scan, immediately sacrifice the mice by carbon dioxide asphyxiation and confirm the deaths by pinching the paws of the animals. Once confirmed, perform cervical dislocations.
6. Remove the blood in mouse tissues by first cutting open the right atrium and then injecting 20 mL PBS into the left ventricle, and subsequently collect the relevant tissues such as tumor, liver, spleen, lung, kidney, muscle, and others [16].

7. Weigh the tissues, measure their radioactivity content by gamma counting [8, 9], and calculate the tissue radioactivity accumulation as a percentage of the injected dose per g (%ID/g).

3. *Ex Vivo* Flow Cytometry and Immunostaining

NOTE: Inject about 100 µL of fluorescent liposomes into melanoma mice through their tail vein at a dose of 0.5 mg of dye per kg of body weight. If radioactive samples are not allowed in the flow cytometer and fluorescence microscope, non-radioactive liposomes must be used.

1. Sacrifice the mice 24 h post injection, as in step 2.5, and collect the tumors, which must be stored in cold PBS.
2. For flow cytometry, follow these steps [17]:
    1. Prepare an enzyme cocktail consisting of a mixture of purified collagenase I and II (4 U/mL), hyaluronidase (60 U/mL), and DNase I (60 U/mL) in flow cytometry buffer (PBS with 0.5% BSA and 1 mM EDTA).
    2. Mix 100 mg of tumor tissue with 200 µL of enzyme cocktail buffer in a 1.5-mL tube and dice the tissue to small pieces with fine scissors. Add another 1.3 mL of enzyme cocktail into the tube and transfer its contents to a 6-well plate.
    3. Shake the 6-well plate on a horizontal shaker placed inside a 37 °C oven for 60 min at 60 rpm.
    4. Wash the tissue homogenate with flow cytometry buffer 3 times to obtain a single cell suspension.
    5. Stain the cells with a cocktail of antibodies specific to biomarkers including CD45, CD11b, Ly6C, CD11c, CD64, CD3, MHCII, and CD31 (1:200 dilution for all antibodies; clone information is provided in the materials spreadsheet). Identify relevant cell types and determine their mean fluorescence intensity (MFI) of DiIC12(5)-DS in each cell population with an appropriate flow cytometry analysis software.

3. For immunostaining, follow these steps:
    1. Place a tumor into a cassette filled with optimal cutting medium (OCT) and freeze it on dry ice.
    2. Make 6-µm frozen sections from tumor tissue and place them on histology glass slides; the sections should cover the largest cross-sections of the tumor, which provide the most representative information on the tissue.
    3. Stain the biomarkers (*e.g.,* CD31 for endothelial cells) of interest with the corresponding antibodies (*e.g.,* anti-CD31, clone MEC13.3). Fix the sections with paraformaldehyde; block them with serum matching the species origin of the secondary antibodies; incubate with primary antibodies for 12 h at 4 °C and then with secondary antibodies for 2 h; and finally, wash with PBS and cover with cover slips. Image the stained slides with a Leica upright confocal SP5 microscope [13, 16].

Representative Results

Figure 1 shows an overview of the procedure. **Figure 2** presents the schematic synthesis procedure of the dual-labeled liposomes described in step 1[10]. **Figure 3** displays a representative PET-CT image (**Figure 3a**), radioactivity quantification from PET imaging (**Figure 3b**), blood half-life (**Figure 3c**), and biodistribution (**Figure 3d**) of radioactive nanoparticles, as described in step 2. In **Figure 3a**, the liposomes highly accumulate in the tumor, which is confirmed by the quantification of the imaging results in **Figure 3b**. Furthermore, liposomes show a blood half-life of around 10 h in **Figure 3c**. The *ex vivo* biodistribution confirms the high tumor accumulation of liposomes. Finally, **Figure 4** provides a typical gating procedure to identify relevant cells in a tumor for the single-cell level analysis of nanoparticle accumulation (**Figure 4a** and **b**), which displays the preferential accumulation of the nanoparticle in tumor-associated macrophages (TAM). A representative confocal microscopy image also shows the overlap between nanoparticles and endothelial cells (**Figure 4c**).

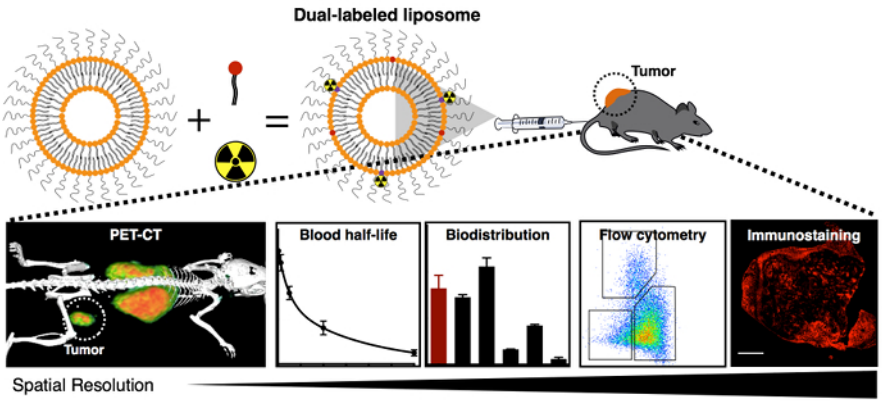

Figure 1. Schematic Overview of the *In Vivo* Nanomedicine Characterization Procedure. This procedure includes the labeling of nanoparticles with both radioactive and fluorescent tags; the characterization of radiolabeled nanoparticles with PET-CT imaging, blood half-life measurements, and biodistribution evaluations; and the single-cell and sub-cellular analysis of fluorescent nanoparticles by flow cytometry and immunostaining, respectively. The techniques, from left to right, provide increasing spatial resolution of nanoparticle *in vivo* accumulation. Please click here to view a larger version of this figure.

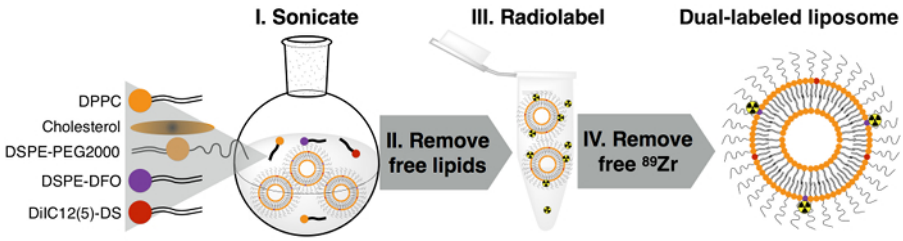

Figure 2. Synthesis Procedure of Dual-labeled Liposomes. Please click here to view a larger version of this figure.

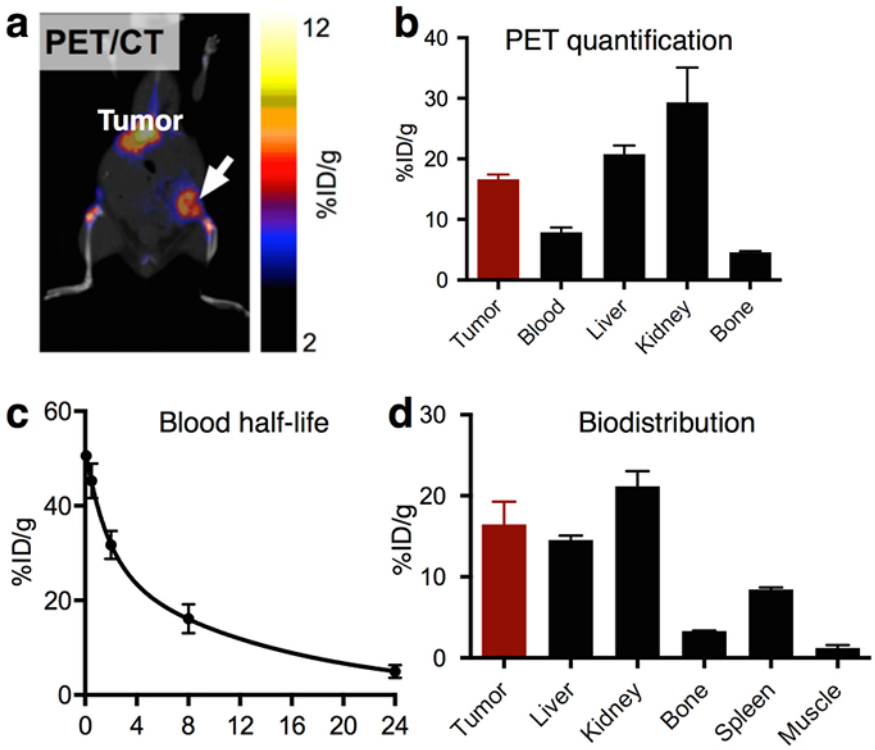

Figure 3. Representative Results of *In Vivo* Characterization of Radiolabeled Nanoparticles. (a) PET-CT images of a tumor-bearing mouse after nanoparticle injection and **(b)** PET-derived uptake values in multiple tissues (n = 3). **(c)** Blood radioactivity half-life of a radiolabeled nanoparticle, as well as **(d)** its biodistribution at 24 h post injection (n = 3). The error bars are the standard deviation. Modified from reference 8, with permission. Please click here to view a larger version of this figure.

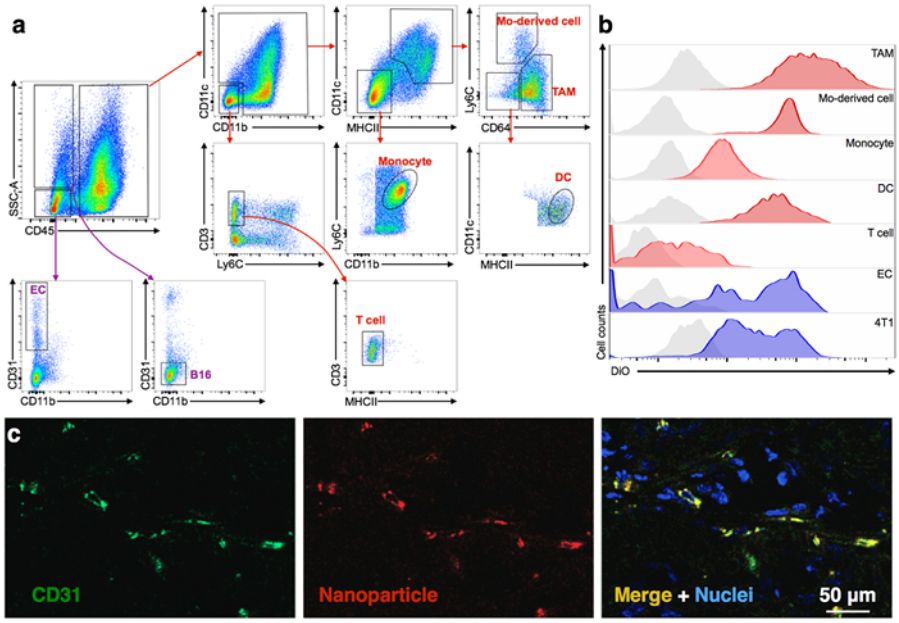

Figure 4. Representative Results of the *In Vivo* Characterization of Fluorescent Nanoparticles. (a) A typical flow cytometry gating procedure to identify tumor-associated immune cells, tumor cells, and endothelial cells (EC), as well as **(b)** the quantification of nanoparticle accumulation in these cells[8]. A representative image of 3 biological repeats. **(c)** Representative immunofluorescence image showing the specific targeting of an RGD-conjugated nanoemulsion to endothelial cells in tumors[13]. Modified from references 8 and 13, with permission. Tumor-associated macrophage (TAM). Please click here to view a larger version of this figure.

Discussion

Critical Steps within the Protocol:

The high quality of dual-labeled liposomes is the key to producing consistent results over a long period of time. Free fluorescent dyes or ^{89}Zr ions can generate totally different targeting patterns and must be completely removed during the purification step. In addition, if the immune system significantly affects experimental cancer nanomedicine performance, the use of immunocompetent mouse models should be preferable, such as the B16-F10 melanoma model in C57BL/6 mice, which was used throughout this protocol. If the tumor microenvironment or a particular combination of genetic mutations is a major factor, patient-derived tumor xenograft models would be ideal choices.

Modification and Troubleshooting:

Our procedure provides a straightforward and reliable way to evaluate the *in vivo* performance of nanomedicines in tumor-bearing animals. This procedure serves as a backbone to build specific experiments to characterize cancer nanomedicines for different applications. For example, researchers can determine quantitative *in vivo* pharmacokinetics of the nanomaterial when PET-CT scans are performed at multiple time points on the same animals[17]; they can collect biodistribution information of the nanomaterials by analyzing other tissues, such as the large intestines, small intestines, pancreas, brain, skin, thymus, stomach, or salivary glands, as shown in other publications[18,19,20,21]; or they can evaluate the single-cell and subcellular specificity of nanomedicines in relevant tissues other than tumors by applying this flow cytometry and immunostaining protocol.

Limitations of the Technique:

This protocol requires some specialized research infrastructure-including radiochemistry and imaging facilities-and technical expertise in radiolabeling, small-animal imaging, and immunology. Therefore, it would be ideally executed by a multidisciplinary team of researchers with expertise in the relevant fields. Our own experience shows that the optimal execution of this procedure requires careful planning and efficient collaboration.

It is worth noting that the specific protocols and proposed agents in this manuscript are best suited for radiolabeling lipid-based nanoparticles. However, the concept of dual-labeled nanoparticles can be employed to characterize other nanoparticle formulations that are, for example, based on gold nanocrystals, polymers, or even viral particles. In these cases, different labeling strategies will be required. It is important to emphasize the wide variety of radioactive isotopes used in biomedical imaging, including ^{89}Zr, ^{18}F, ^{64}Cu, ^{68}Ga, and ^{123}I, to name just a few[7]. The choice of radioisotope must be made based on the specific properties of the nanomaterial under investigation, chiefly its blood circulation half-life, to allow for full characterization at later time points. However, other factors, such as labeling chemistry or isotope availability, may influence the final selection. For this study, ^{89}Zr was chosen because its long physical half-life ($t_{1/2}$ = 78.4 h) is comparable to the blood half-life of liposomes. Of note, this protocol can also be performed with other isotopes, like ^{99m}Tc, ^{111}In, or ^{125}I, that are commercially available and suitable for imaging with single-photon emission computed tomography (SPECT). Similarly, DiIC was chosen due to its high hydrophobicity and therefore high loading efficiency in liposomes. Other fluorescent dyes with unfavorable physicochemical properties can be directly conjugated to the phospholipids[17].

Significance of the Techniques:

This procedure presents high translational potential when adapted to evaluate nanomedicines in clinical studies. The 4 key techniques-namely, PET-CT imaging, radioactivity measurement, flow cytometry, and immunohistochemistry-are routinely used for oncological diagnosis in patients. Therefore, this preclinical procedure can be easily translated to evaluate the *in vivo* performance of nanomedicines in the clinical phase. Furthermore, the larger size of human organs compared to mice allows for more accurate analysis by PET-CT imaging[22], which can replace the invasive biopsy-based radioactivity measurement of nanomedicine accumulation. In this setting, non-invasive, imaging-guided protocols can be developed to stratify patients and to help homogenize patient outcome[10]. Developing radioactive nanomaterials still requires a substantial infrastructure investment. Alternatively, non-radioactive imaging techniques based on magnetic resonance imaging (MRI) have been rapidly evolving in the past decade. For example, magnetic particle imaging (MPI) uses small iron oxide nanoparticles (10 to 20 nm) and could provide much more quantitative evaluation of nanomedicines labeled with iron oxide nanoparticles *in vivo* than the current MRI techniques[23]. Clinical translation of MPI would allow more researchers to use robust *in vivo* imaging techniques to evaluate the *in vivo* performance of cancer nanomedicines.

Future Applications:

Once researchers master these protocols, they can apply the procedures to characterize most fluorescent and radioactive dual-labeled, novel materials, including peptides, proteins, antibodies, antibody fragments, and so forth. These procedures can help scientists to thoroughly evaluate the *in vivo* performance of novel biomedical materials and to identify those with great translational potential.

In conclusion, we aim to introduce a comprehensive nanomedicine characterization procedure that can provide systemic, tissue, single-cell, and subcellular level nanomedicine accumulation information. Currently, the majority of cancer nanomedicines still fail in Phase I clinical trials due to their suboptimal pharmacokinetics, biodistributions, and toxicity profiles. On the other hand, the great heterogeneity of therapy response to nanomedicine mandates a companion imaging strategy for selecting patients who may particularly benefit from these experimental nanomedicines. We believe that the adoption of this procedure could help the community to identify promising nanomedicines with high translational potential in preclinical animal models and, with the proper modification, could also help clinical researchers to identify patients amenable to nanotherapy.

Disclosures

The authors have no disclosure to make.

Acknowledgements

The authors would like to thank Drs. Helene Salmon and Miriam Merad from Icahn School of Medicine at Mount Sinai for providing the B16-F10-YFP cells and for their expert advice on melanoma mouse models. The authors further thank the Animal Imaging Core Facility, the Radiochemistry and Molecular Imaging Probes Core Facility, and the Molecular Cytology Core Facility at Memorial Sloan Kettering Cancer Center (MSK) for their support. This work was supported by National Institutes of Health grants NIH 1 R01 HL125703 (W.J.M.M.), R01CA155432 (W.J.M.M.), K25 EB016673 (T.R.) and P30 CA008748 (MSK Center Grant). The authors also thank the Center for Molecular Imaging and Nanotechnology (CMINT) at MSK for their financial support (T.R.).

References

1. Peer, D. *et al.* Nanocarriers as an emerging platform for cancer therapy. *Nat Nanotechnol.*, 2, 751-60 (2007).
2. Barenholz, Y. Doxil(R)--the first FDA-approved nano-drug: lessons learned. *J Control Release.*, 160, 117-34 (2012).
3. Green, M. R. *et al.* Abraxane, a novel Cremophor-free, albumin-bound particle form of paclitaxel for the treatment of advanced non-small-cell lung cancer. *Ann Oncol.*, 17, 1263-8 (2006).
4. Juliano, R. Nanomedicine: is the wave cresting? *Nat Rev Drug Discov.*, 12, 171-2 (2013).
5. Ledford, H. Bankruptcy filing worries developers of nanoparticle cancer drugs. *Nature.*, 533, 304-5 (2016).
6. Venditto, V. J.; Szoka, F. C., Jr. Cancer nanomedicines: so many papers and so few drugs! *Adv Drug Deliv Rev.*, 65, 80-8 (2013).
7. Dunphy, M. P.; Lewis, J. S. Radiopharmaceuticals in preclinical and clinical development for monitoring of therapy with PET. *J Nucl Med.*, 50 Suppl 1, 106S-21S (2009).
8. Perez-Medina, C. *et al.* PET Imaging of Tumor-Associated Macrophages with 89Zr-Labeled High-Density Lipoprotein Nanoparticles. *J Nucl Med.*, 56, 1272-7 (2015).
9. Perez-Medina, C. *et al.* A modular labeling strategy for in vivo PET and near-infrared fluorescence imaging of nanoparticle tumor targeting. *J Nucl Med.*, 55, 1706-11 (2014).
10. Perez-Medina, C. *et al.* Nanoreporter PET predicts the efficacy of anti-cancer therapy. *Nature communications.* (2016).
11. Tang, J. *et al.* Inhibiting macrophage proliferation suppresses atherosclerotic plaque inflammation. *Science advances.* (2015).
12. Priem, B.; Tian, C.; Tang, J.; Zhao, Y.; Mulder, W. J. Fluorescent nanoparticles for the accurate detection of drug delivery. *Expert Opin Drug Deliv.*, 12, 1881-94 (2015).
13. Gianella, A. *et al.* Multifunctional nanoemulsion platform for imaging guided therapy evaluated in experimental cancer. *ACS Nano.*, 5, 4422-33 (2011).
14. Torchilin, V. P. Recent advances with liposomes as pharmaceutical carriers. *Nat Rev Drug Discov.*, 4, 145-60 (2005).
15. Salmon, H. *et al.* Expansion and Activation of CD103(+) Dendritic Cell Progenitors at the Tumor Site Enhances Tumor Responses to Therapeutic PD-L1 and BRAF Inhibition. *Immunity.*, 44, 924-38 (2016).
16. Perez-Medina, C. *et al.* In Vivo PET Imaging of HDL in Multiple Atherosclerosis Models. *JACC Cardiovasc Imaging.*, 9, 950-61. (2016).
17. Duivenvoorden, R. *et al.* A statin-loaded reconstituted high-density lipoprotein nanoparticle inhibits atherosclerotic plaque inflammation. *Nature communications.*, 5, 3065 (2014).

18. Carney, B. *et al.* Non-invasive PET Imaging of PARP1 Expression in Glioblastoma Models. *Mol Imaging Biol.* (2015).
19. Salinas, B. *et al.* Radioiodinated PARP1 tracers for glioblastoma imaging. *EJNMMI Res.*, 5, 123 (2015).
20. Carlucci, G. *et al.* Dual-Modality Optical/PET Imaging of PARP1 in Glioblastoma. *Mol Imaging Biol.*, 17, 848-55 (2015).
21. Tang, J. *et al.* Immune cell screening of a nanoparticle library improves atherosclerosis therapy. *Proc. Natl. Acad. Sci. USA.* (2016).
22. Scott, A. M.; Wolchok, J. D.; Old, L. J. Antibody therapy of cancer. *Nat Rev Cancer.*, 12, 278-87 (2012).
23. Goodwill, P. *et al.* X-space MPI: magnetic nanoparticles for safe medical imaging. *Adv Mater.*, 24, 3870-7 (2012).

